JTTEE5 18:546–554
DOI: 10.1007/s11666-009-9324-3
1059-9630/$19.00 © ASM International

Gas Dynamic Principles and Experimental Investigations of Shock Tunnel Produced Coatings

X. Luo and H. Olivier

(Submitted January 6, 2009; in revised form February 28, 2009)

For enhancing coating quality, the shock tunnel technology is employed to increase impact velocities of particles up to 1,500 m/s for 10-μm solid particles. Based on a parametric study, an experimental facility has been set up at the Shock Wave Laboratory (SWL) of RWTH Aachen University. A calibration of the nozzle flow has been carried out using a Pitot rake. The conditions in the reservoir achieved so far are $p_0 = 140$ bar and $T_0 = 1{,}800$ K. A high-speed schlieren system is set up for flow visualization and also for velocity measurement of visible particles. For fine particles, both LDA and PIV methods are used for particle velocity measurements. The results achieved are in good agreement with a quasi-1D prediction. The quality of a first coating sample of copper on a steel substrate is analyzed which shows a promising improvement. Systematic experiments have to be carried out with different material combinations of coating and substrate, different particle velocities, and temperatures for further evaluation of this technique.

Keywords cold gas-dynamic spray, particle impact velocity, particle velocity measurement, shock tunnel

1. Introduction

Thermal spray processes such as plasma spraying, arc spraying, and high-velocity oxy-fuel spraying (HVOF) are widely used for modern coating applications. Depending on the desired coating properties and the used material, different coating techniques are used. For example, to produce highly porous ceramic thermal barrier coatings, the atmospheric plasma spraying can be applied because this technique can provide the powder with high thermal and kinetic energies. Another example is to produce dense, highly homogeneous protective coatings against wear or oxidation as well as for the deposition of electrical insulators. In this case, metallic and ceramic materials are mostly used and high kinetic energies combined with low temperatures are needed, which can be provided by the HVOF. The energy required for a good particle-surface adhesion is provided by the high kinetic energy which is efficiently transferred into the bond strength during impact. Moderate temperatures and almost no-oxidation processes lead to small metallurgical changes in the powder properties and also a low thermal load of the substrate (Ref 1). High temperatures in thermal spraying may cause detrimental effects such as oxidation, phase transformations, or crack formation due to the stresses introduced during rapid solidification of the spray material on the substrate, and therefore, lower the coating performance (Ref 2). Within the last three decades, major developments evolved with an aim to lower the process temperatures and increase gas and particle velocities. These crucial requirements for higher particle velocities and lower operation temperatures imposed have led to the continuous development of the cold gas dynamic spraying (CGDS) technology (Ref 3-8), where process temperatures are far below the melting point of respective spray materials. This continuous combustion-free process, mostly driven with the use of inert gases, is largely applicable for ductile and oxidation sensitive materials. The higher velocities and lower temperatures, compared with the HVOF process, allow a homogeneous deformation of the powder particles at the surface (no breaking) resulting in an outstanding bond strength at the coating-substrate interface.

The CGDS process basically uses the energy stored in a high-pressure compressed gas to accelerate fine powder particles to very high velocities in a range between 500 and 1000 m/s (Ref 9). According to the prevailing theory for cold-spray bonding (Ref 10), bonding occurs only when the particle velocities exceed a minimum critical velocity. This critical velocity depends not only on the type of spraying and substrate material but also on the particle size and the particle temperature on impact. Schmidt et al. (Ref 11) developed a generalized parameter window for cold-spray deposition by defining the influences of particle temperature and velocity on bonding. It is desirable to further increase the impact velocity of particles to enhance the quality of the CGDS and to extend the application range of the CGDS. The development of unsteady

X. Luo, Department of Modern Mechanics, University of Science and Technology of China, Hefei 230026, People's Republic of China and Shock Wave Laboratory (SWL), RWTH Aachen University, Aachen, Germany; and **H. Olivier**, Shock Wave Laboratory (SWL), RWTH Aachen University, Aachen, Germany. Contact e-mail: xluo@ustc.edu.cn.

cold-spraying processes for the achievement of higher quality coating is a recent research topic. For example, a concept for a pulsed-cold gas dynamic process is presented in Ref 12, which adopts the shock tube technology. Because pre-heated particles are injected just after the passage of the shock, this process could allow the feedstock particles to be accelerated to high impact velocities and intermediate temperatures (below melting temperature). In this way, the intermediate particle impact temperature would lead to lower required critical velocities compared to conventional CGDS.

We proposed another new concept for the cold gas-dynamic spray technique (Ref 13, 14), which increases the solid particle velocity up to 1500 m/s and, at the same time, keeps particle temperatures low to moderate. This method uses the super-to-hypersonic shock tunnel technology to generate a reservoir condition with high temperature and high pressure. The particles are injected into the nozzle flow downstream of the nozzle throat after the nozzle flow is fully established. The optimal choice of the process parameters can provide high quality coatings deposited at low temperatures. In order to build up a thick coating layer using this technique, an intermittent operation is necessary. A theoretical model based on gas-particle flows is also presented in Ref 15 to describe the behavior of the flow and the diluted solid particles during the modified cold-spray process. This quasi-1D model is capable to consider non-equilibrium effects of the gas phase due to high reservoir temperatures, and the influence of wall friction and heat transfer.

We shall first discuss the gas dynamic principles of this new concept for coating application, where several problems will be described and solutions for them are also be given. Then, the supersonic nozzle design by a parametric study and other components of the experimental facility are outlined. Measuring setups and methods for measuring pressure, heat flux, and particle velocity are also briefly discussed. In section 4, the flow calibration is described, first carried out in this facility without particles to determine the free stream conditions as well as the reservoir conditions. Then, particles are injected into the established nozzle flow and measurements of particle velocities are performed. Finally, a first coating test is carried out by spraying copper powder on a steel substrate. Conclusions are drawn in section 5.

2. Gas Dynamic Principles

2.1 Concept

The gas dynamic principle of this new concept is sketched in Fig. 1, which basically adopts the shock tunnel technology. Initially, the high pressure section (HPS) and the double diaphragm chamber (DD) are filled with compressed gas to desired pressures. The low pressure section (LPS), the supersonic nozzle (N), and the dump tank (DT) are filled with nitrogen to atmospheric pressure. Then, the release valve is opened, which causes a quick drop of the pressure in the DD. As a consequence,

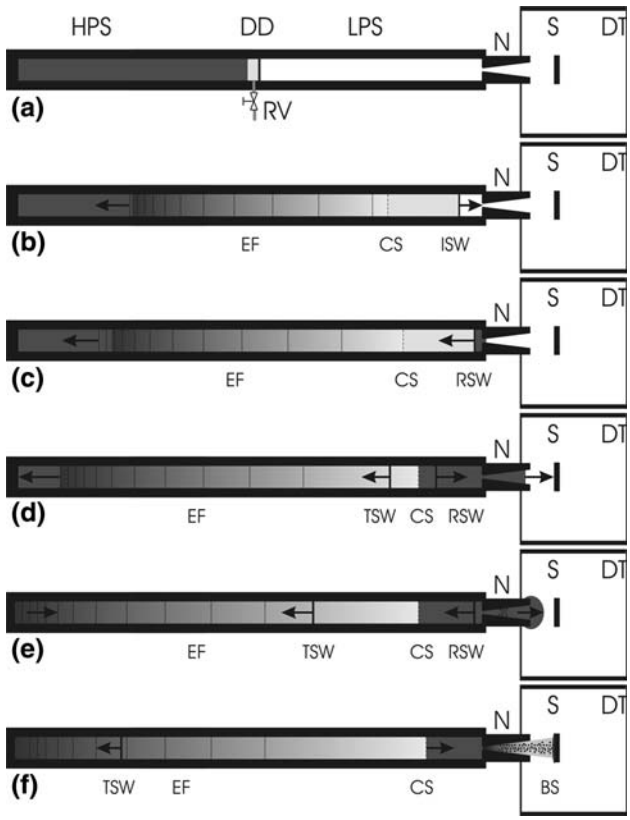

Fig. 1 Schematic of one shot of shock tunnel produced cold spray. HPS: high pressure section, LPS: low pressure section, DD: double diaphragm chamber, N: nozzle, S: substrate, DT: dump tank, RV: release valve, EF: expansion fan, CS: contact surface, ISW: incident shock wave, RSW: reflected shock wave, TSW: transmitted shock wave, BS: bow shock

diaphragms are ruptured and a shock wave (ISW) is formed running into the LPS. At the same time, an expansion fan (EF) is generated, which travels upstream into the HPS. A contact surface (CS) is also created, which separates a high-temperature-flow zone behind the shock wave from a low-temperature-flow zone caused by the expansion wave. Gases in these two zones have the same pressure and velocity. When the shock wave hits the entrance of the supersonic nozzle, it is almost fully reflected due to the very small entrance and the very small throat size of the nozzle. The reflection leads to a high temperature and pressure in the region between the entrance of the nozzle and the reflected shock wave (RSW), which can be considered as the reservoir. When the RSW interacts with the contact surface, different interaction patterns may occur depending on the gas properties in these two regions. In this concept, the over-tailored operation is used, in which a RSW and a transmitted shock wave (TSW) are generated in the interaction. The right-running RSW from the contact surface is again fully reflected from the entrance of the nozzle, and again interacts with the contact surface. During the interaction, the strength of the shock decreases and finally a nearly stable reservoir condition is created. It should be noted that the multi-reflection process leads

to a further increase of the reservoir conditions, i.e., higher temperature, density, and pressure. The supersonic nozzle flow starts when the incident shock wave passes through the nozzle and after a very short period of the starting process a quasi-stable nozzle flow is established. Then the particles are injected into and accelerated by the established nozzle flow. Due to high velocities of the particles, a dense coating layer is expected on the substrate, which is mounted at a short distance from the nozzle exit.

2.2 Problems and Corresponding Solutions

In order to lower the particle temperatures, the particles are injected downstream of the nozzle throat, which means that the nozzle should have a sufficient length so that there is a sufficient acceleration distance for the particles to achieve high velocities. As a consequence, the influence of the boundary layer becomes significant. Furthermore, the exit Mach number will increase for longer nozzles.

In this concept, the LPS of the shock tube connected to the nozzle is filled with nitrogen to atmospheric pressure. The nozzle flow pattern depends on the ratio between the reservoir pressure and the dump tank pressure. To ensure a shock-free nozzle flow, a high reservoir pressure or a low dump tank pressure is needed. The gas in the LPS will be compressed and heated up by the shock system and function as the working media. For a given filling pressure, the volumes of the LPS and the nozzle throat size determine the useful spraying time. In order to ensure a sufficient spraying time and the start of the nozzle, a second diaphragm can be mounted between the LPS and the nozzle. Then, the pressure in the LPS can be kept as 1 bar, while the nozzle and the dump tank can be evacuated.

The injection of the particles requires special attention because the particles have to be injected at the right instant of time, i.e., neither too early and nor too late after the flow initiation process. Furthermore, a good mixing of the particles with the flow is necessary because the particles are injected into s supersonic flow, and the particle injection needs a high pressure to overcome the pressure in the flow. The possible way to fulfill these requirements is to adopt a by-pass tube which uses the high pressure gas in the reservoir to introduce the particles into the supersonic nozzle flow.

3. Experimental Setup and Measuring Techniques

A quasi-1D method has been developed to describe the behavior of the flow and the diluted solid particles during the modified cold-spray process (Ref 15), which is capable to consider non-equilibrium effects of the gas phase due to high reservoir temperatures, and the influence of wall friction and heat transfer averaged over the nozzle cross section. By a detailed parametric study considering the influence of the expansion rate, the stagnation temperature and pressure, the injection position, and the particle diameter, the optimized conical nozzle geometry has been obtained to generate high particle velocities for coating applications. Based on this parametric study (Ref 15), a nozzle with optimized performance has been chosen resulting in a conical nozzle with a half opening angle of 2.8^{o} and a length of 320 mm. The throat diameter amounts to 7.8 mm, and the exit diameter measures to 39.7 mm. The particle injection device is fixed in the LPS of the shock tube and extends into the supersonic nozzle part. For this, a small tube (outer diameter 3.0 mm, inner diameter 1.2 mm) reaches into the divergent nozzle part so that the injection position is about 52 mm downstream of the throat.

The shock tube has an outer diameter of 108 mm and an inner diameter of 56 mm. This tube is made of stainless steel and is able to sustain very high pressures up to 1000 bar. A schematic drawing of the setup is shown in Fig. 2. The shock tube has a HPS of 3.3 m and a LPS of 3.5 m length.

In order to determine the free stream flow conditions downstream of the nozzle exit, a Pitot rake (see Fig. 3) is used, which consists of five Pitot tubes connected with five Kulite pressure transducers and a sphere installed with a coaxial thermocouple at its stagnation point. The reservoir

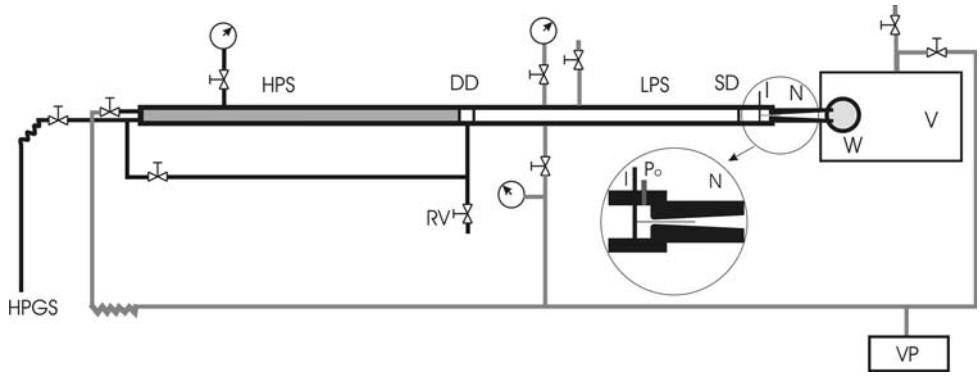

Fig. 2 Schematic drawing of the shock tunnel with peripheries. HPGS: high pressure gas supply, HPS: high pressure section, DD: double diaphragm chamber, LP: low pressure section, I: injection device, N: nozzle, W: test window, V: vacuum tank, VP: vacuum pump, SD: second diaphragm

pressure is directly measured by a Kistler pressure transducer mounted shortly upstream of the nozzle entrance. The reservoir temperature and free stream conditions are derived from the heat flux deduced from the thermocouple signal, the Pitot pressure, and the static pressure employing the method described in Ref 16.

A schlieren system is set up for flow visualization, which allows taking 16 schlieren photos in one experiment with a time interval between two successive photos of down to 1 μs, which is also very useful for the determination of the velocity of visible particles.

For velocity measurements of fine particles, a laser Doppler anemometer (LDA) system and a particle imaging velocimetry (PIV) system have been set up. In order to measure very high particle velocities, a very small angle is used in the LDA system, which results in a measurement volume of $17 \times 0.16 \times 0.16$ mm^3.

For the PIV measurements, a holographic double-pulse laser system (JK Laser system 2000) with a pulse separation time in the microsecond range is adopted to create a laser light sheet (thickness 0.5 mm) perpendicular to the nozzle axis. A Kodak Megaplus ES1 CCD camera is employed to acquire either two images in two frames or one double exposure image in a single frame within a pulse delay in the microsecond range. The image data is then analyzed with the PIV software to obtain the particle velocity field.

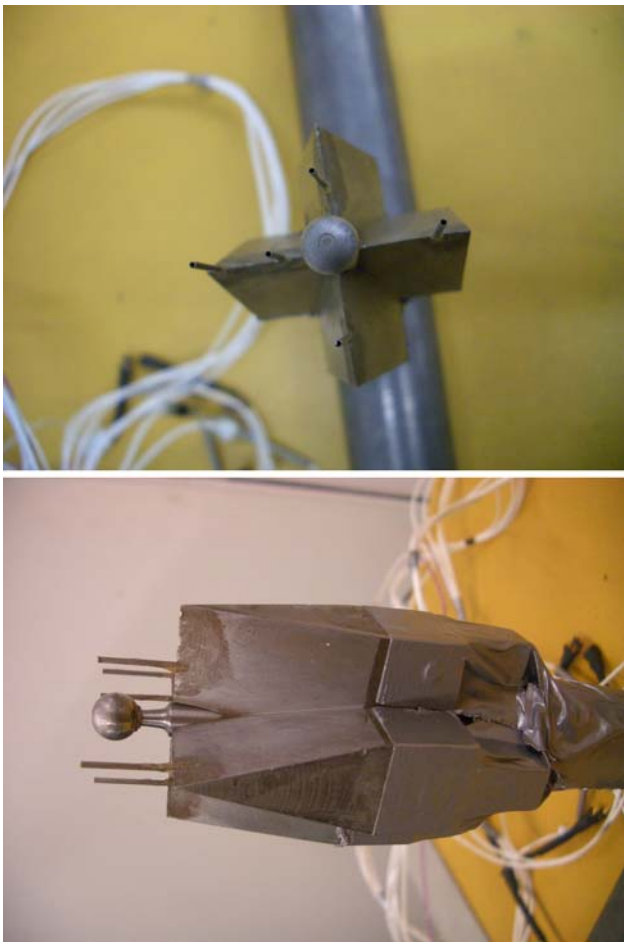

Fig. 3 Photos of Pitot rake which consists of a thermocouple sphere and five Pitot tubes

4. Results and Discussions

4.1 Flow Calibration

Measured temperature and pressure histories in the reservoir are shown in Fig. 4. Initially, the HPS is filled with a mixture of helium (partial pressure 140 bar) and air (partial pressure 170 bar), and the LPS is at atmospheric pressure. A pre-cut copper diaphragm of 0.5-mm thickness is mounted at the end of the LPS, and the dump tank is

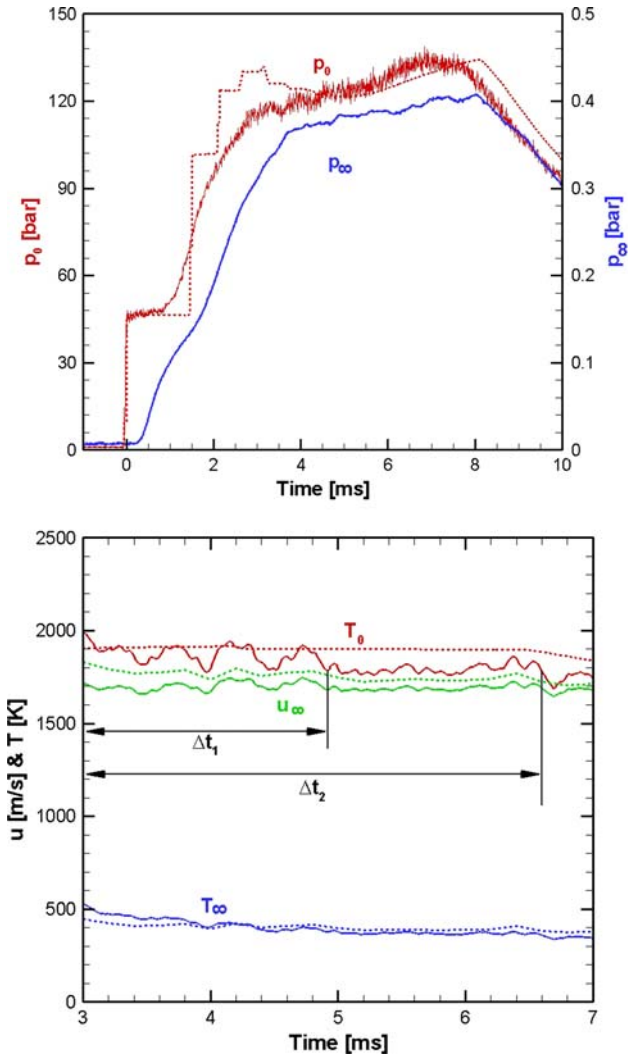

Fig. 4 Experimental results (*solid lines*) and corresponding numerical results (*dotted lines*). Reservoir pressure p_0 and static pressure histories p_∞ (*upper*); deduced reservoir temperature T_0, free stream velocity u_∞, and temperature T_∞ (*lower*). Initial condition: $p_4 = 310$ bar (partial pressure of helium 140 bar, partial pressure of air 170 bar), $p_1 = 1$ bar

evacuated to a low pressure of about 180 Pa. The shock tube simulation code KASIMIR (Ref 17) has been utilized for the comparison of the experimental results with the theoretical prediction, shown as dotted lines, in which equilibrium gas effects are taken into account in KASIMIR. It should be mentioned that KASIMIR is well validated for ideal shock tube experiments, and it is improved by using a user-specific gas model of the mixture of helium and air in KASIMIR to more precisely simulate real-gas effects behind the RSW. The reservoir temperature in the experiment slightly decreases with time and the testing time is about 2 ms for $T_0 \geq 1800$ K (Δt_1) and 4 ms for $T_0 \geq 1700$ K (Δt_2), respectively.

Some typical Pitot pressure histories measured by the Pitot rake in one experiment are shown in Fig. 5(a), together with the total pressure measured in the reservoir and the static pressure at the exit of the nozzle. The lowest one of the Pitot pressure signals corresponds to the transducer located outmost from the jet center. By changing the transverse position of the Pitot rake from shot to shot, the Pitot pressure profile along the radius of the nozzle exit has been obtained, see Fig. 5(b). The Pitot pressure is scaled by the actual reservoir pressure because the reservoir pressure slightly varies for different experiments. Each point in this figure represents an average value over the testing time. This Pitot pressure profile clearly indicates that the core flow region of the jet ($0 < r < 14$ mm) is repeatable from shot to shot.

Figure 5(c) provides an experimental as well as theoretical relation of the reservoir temperature with the shock speed by KASIMIR. The relatively large scattering of the experimental data in Fig. 5(c) is due to the partial pressure of helium not being the same for all experiments. Furthermore, the filling process of the different gases is not yet optimized and therefore, might cause variations for each experiment. The general deviation between the theoretical and experimental values in Fig. 5(c) is caused by the mixing process taking place at the contact surface between the high- and low-pressure section gas in the experiments. The numerical simulation of the particle-laden nozzle flow by the quasi-1D method and the description of the experimental results are based on the real nozzle reservoir conditions. Therefore, the numerical simulations of the nozzle flow as well as the analysis of the experimental results are performed for the experimental conditions shown in Fig. 5(a) and not for the theoretical ones obtained by the simulation tool KASIMIR. The deviations observed in Fig. 5(a) result from high shock Mach numbers, which are necessary to achieve the desired reservoir conditions. For lower shock Mach numbers, in general, a good agreement is achieved between experimental and theoretical values.

4.2 Particle Velocity Measurement

For first experiments, some big glass spheres (diameter 2.0 mm) were put on a flat surface of the injection device. The particles can be identified in the schlieren photos as shown in Fig. 6. In this case, the particle velocity deduced from the schlieren photos is about 200 m/s. Then, smaller

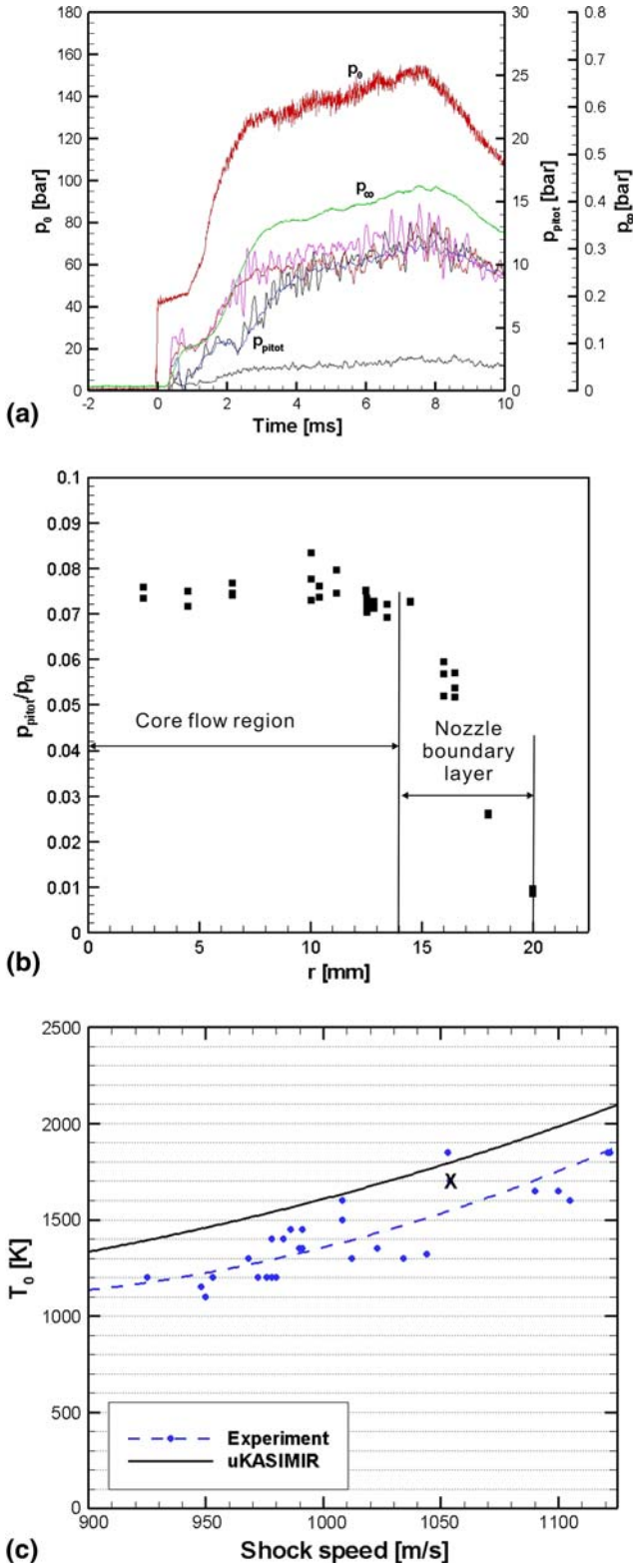

Fig. 5 (a): Typical Pitot pressure histories measured by the Pitot rake. (b) Cross-sectional Pitot pressure profile at the nozzle exit. (c) Relation of the reservoir temperature with the shock speed. *Solid line*: theoretical prediction by KASIMIR, *dashed line*: polynomial fit of experimental data. The experimental point marked by a cross corresponds to the one of Fig. 4

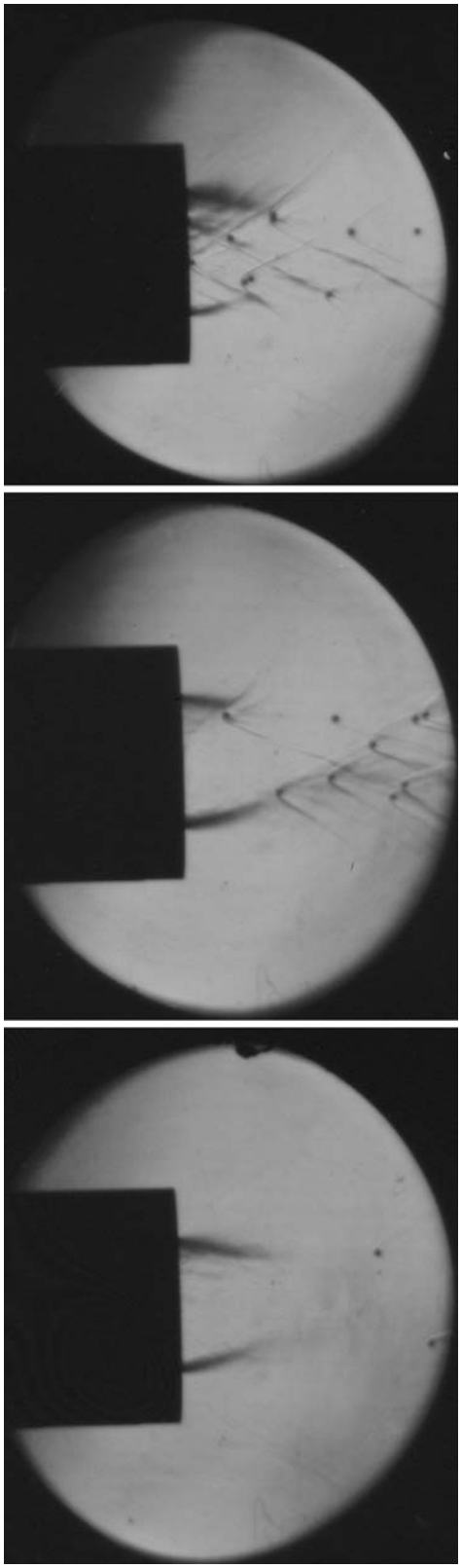

Fig. 6 Schlieren pictures for 2-mm glass spheres added in the nozzle prior to the experiment, pictures taken at 3.30, 3.45, and 3.60 ms, respectively, after flow starting

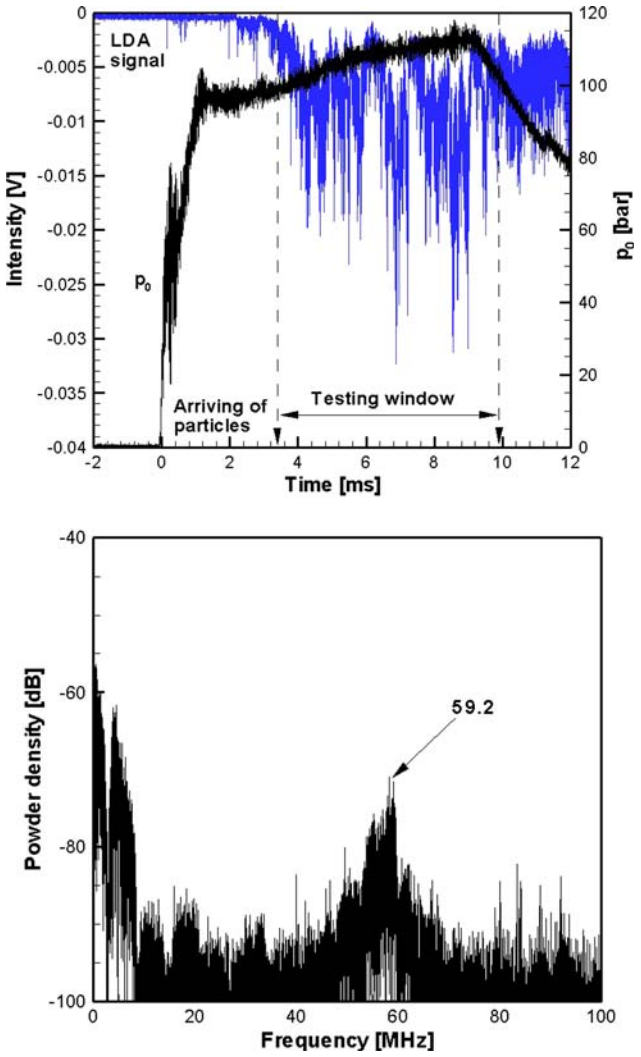

Fig. 7 *Top*: determination of the arriving time of particles by the LDA system, time division 1 ms. *Bottom*: determination of the Doppler frequency by FFT

glass spheres with 0.6-mm diameter have been used. The measured mean particle velocity is about 350 m/s, which is almost the same as given by the theoretical prediction (356.6 m/s) utilizing the quasi-1D code, which has also been used for the parametric study. For this experiment, the reservoir condition is given by $p_0 = 120$ bar and $T_0 = 1800$ K.

For 15-μm stainless steel particles put on a flat surface of the injection device, the arriving time of the particles is first measured by the LDA system with time division of 1 ms, see Fig. 7. It can be found that the particles arrive at the nozzle exit after a delay of 3.5 ms, and the particle flow lasts for several milliseconds. A smaller time division (50 μs) has been used for detailed particle velocity measurements. The mean particle velocity measured by the LDA method is about 1050 m/s for the reservoir condition of $p_0 = 140$ bar and $T_0 = 1800$ K.

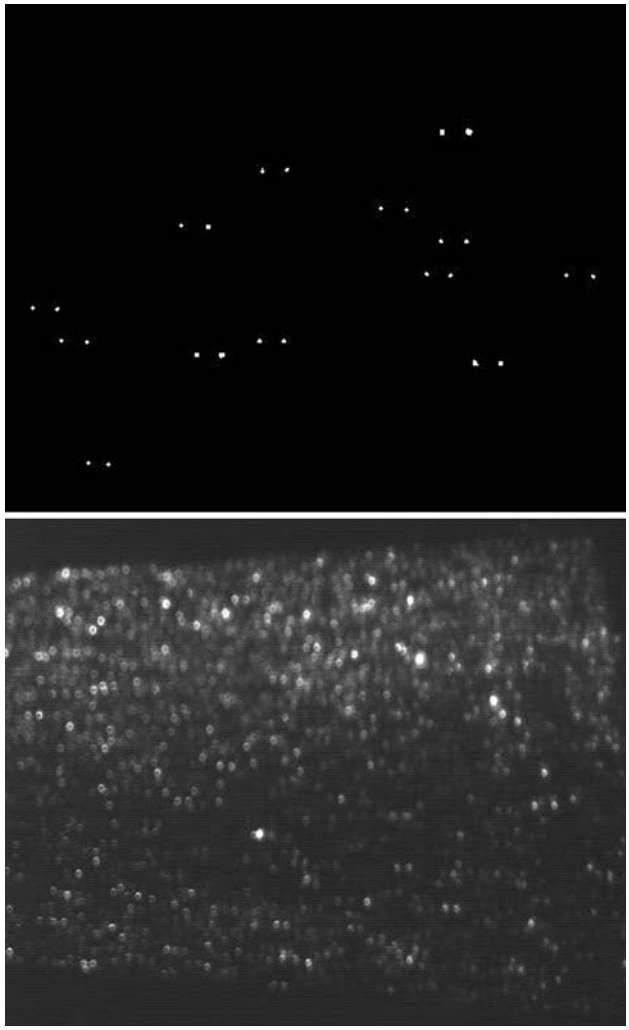

Fig. 8 Double-exposure images in single-frame mode for particles added in the reservoir (*Top*, interval 2.2 μs) and in the injection tube (*Bottom*, interval 1.48 μs). Initial condition: $p_4 = 200$ bar, $p_1 = 1$ bar

Up to now, experiments with PIV are still going on for different conditions. In this article, only preliminary results of the PIV measurements are presented for air as driver gas. Figure 8 shows double-exposure images for the single frame mode for stainless steel particles of mean diameter of 15 μm added in the reservoir (left) and in the injection tube (right). With the use of the particle-pairing method, it is found that the averaged particle velocity is about 1220 m/s in the left image and 890 m/s in the right image. The cross-correlation method can also be used to deduce the velocity field by capturing two images in the double frame mode. The mean particle velocity deduced by the cross-correlation method is about 897 m/s, which is the same as for the particle-pairing method.

4.3 First Coating Sample

Similar to the conventional CGDS, a coating within the new shock tunnel based coating technique is produced by exposing a substrate to the gas-particle flow. The substrate consists of a flat disc with a diameter of 40 mm and is placed 35 mm downstream of the nozzle exit. The typical mass of powder per single spraying operation is about 50 mg. In spite of many experiments being carried out, the results of only three samples are presented here to give a concise overview of the process capabilities.

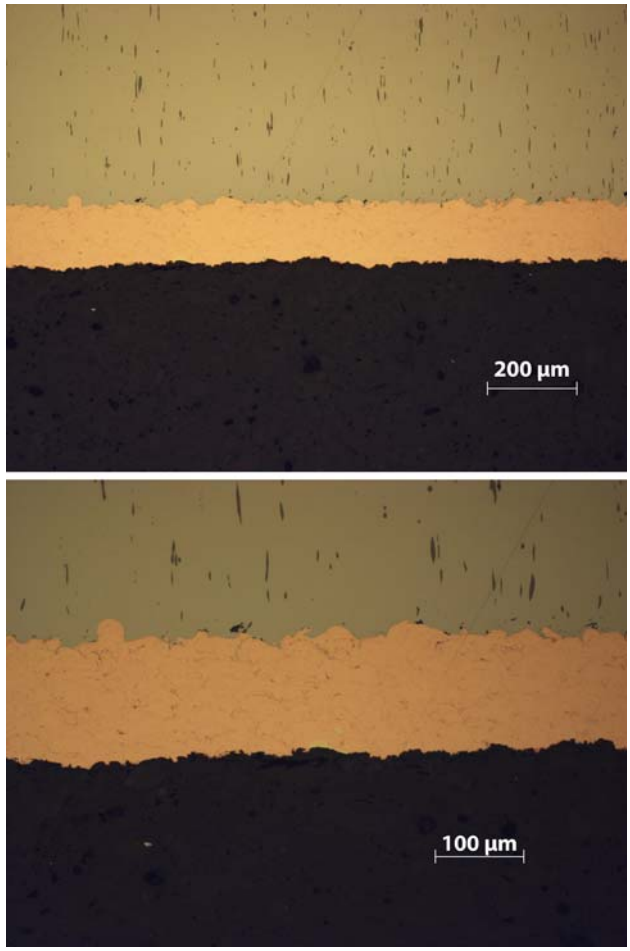

Fig. 9 Cut view of first coating sample. 35-μm copper powder on alumina substrate. Spraying condition: $He/N_2 = 200/1$, particle velocity about 1200 m/s (8 shots)

Figure 9 presents micrographs of sprayed coatings showing the detailed microstructure of copper particles deposited on an alumina substrate. The coating layer has been built up by four successive runs with a particle velocity of 1200 m/s. It can be seen that the coating layer is very dense, and almost no voids are presented.

For the alumina substrate in Fig. 10, the first two shots are made at a high reservoir condition using helium as driver gas, and the last two shots are made at a lower reservoir condition using air as driver gas. The corresponding particle velocities are 1350 and 900 m/s, respectively. We observe that there are some cracks at the interfaces of the coating material deposited by the last two shots. The reason for these cracks is the lower particle velocity of the last shots. However, the first coating layer

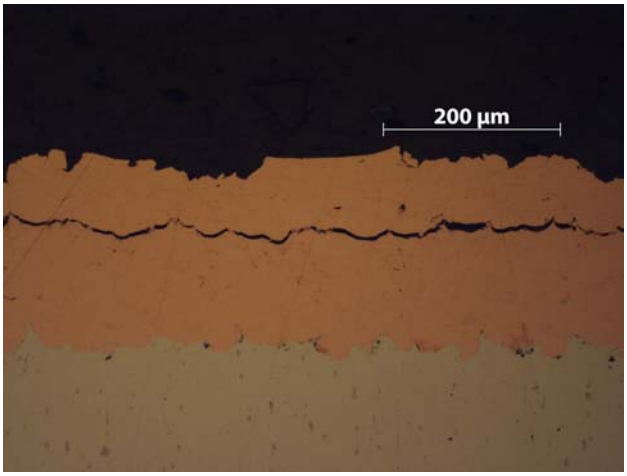

Fig. 10 Cut view of second sample to demonstrate the influence of the particle velocity on coating layer quality, 35-µm copper powder on alumina substrate (4 shots)

produced by the first two shots shows a very low porosity, which indicates a high quality of the layer.

The microstructure of coating samples for copper powder on steel substrate is shown in Fig. 11 for a very high particle velocity (about 1350 m/s measured by LDA). No significant coating layer is found, but erosion may be identified from the very irregular shape of the interface between the coat layer and the substrate, which is hardly found for the previous samples with a good coating layer. Actually by weighing the mass of the substrate after the experiment, a decrease of mass is found. This also suggests that erosion due to very high particle velocity has taken place there. The erosion possibly caused by the high impact particle velocities confirms the theoretical study of Schmidt et al. (Ref 11) and gives an experimental evidence of that.

In general, the coating layers are denser than for the conventional CGDS. It should be noted that there are some voids in both samples. The porosity of the layer amounts to 1.8% for the sample with the higher loading and 1.5% for the one with the lower loading. These results imply that this new technique is able to produce coatings of high quality with dense layers, and low porosity.

5. Conclusions

The shock tunnel technology is employed to achieve particle velocities of more than 1000 m/s for solid particles. A calibration of the nozzle flow has been carried out by using a Pitot rake and a sphere for measuring the stagnation point heat fluxes. The conditions in the reservoir achieved so far are $p_0 = 140$ bar and $T_0 = 1800$ K. A high-speed schlieren system is set up for flow visualization and also for velocity measurements of visible particles. For fine particles, both LDA and PIV methods are used for particle velocity measurements. Results are in good agreement with the theoretical prediction by a quasi-1D method.

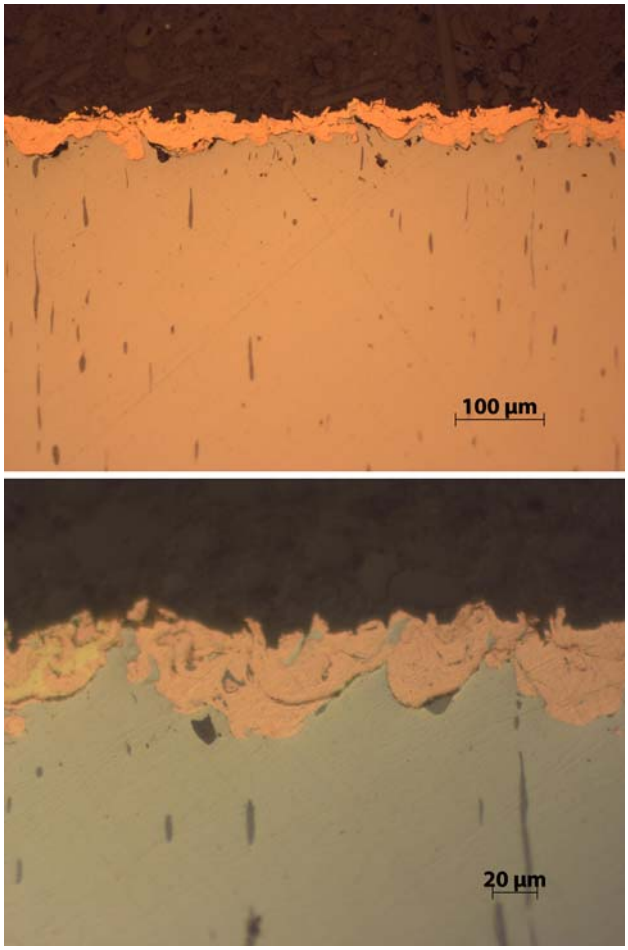

Fig. 11 Cut views of third sample to demonstrate the influence of the particle velocity on deposition. Erosion due to very high particle velocity, 35-µm copper powder on steel substrate (4 shots)

For the existing technologies as of now such as, e.g., plasma coating, the reservoir temperature amounts to 7000 to 20000 K and the pressure to 1 bar, resulting in a typical particle velocity of about 200 to 300 m/s. High particle velocities are achieved with the cold-gas coating technique, where the reservoir temperature is only about 1000 K, but the reservoir pressure about 50 to 100 bar, and the typical particle velocity in the order of 600 to 1000 m/s. This shows that the conditions achieved in this study so far ($p_0 = 140$ bar, $T_0 = 1800$ K, expected copper particle velocity for $d = 10$ µm about 1329 m/s) are already beyond existing technologies. In general, the coating layers produced by the new technology are denser than for the conventional CGDS. The porosity of the layer amounts to 1.5%, which implies that this new technique is able to produce coatings of high quality.

The erosion on the steel substrate possibly caused by the high impact particle velocities confirms the theoretical study of Schmidt et al. (Ref 11) and, for the first time, gives an experimental evidence of that. However, it should be carefully checked to exclude all other possibilities.

For higher particle velocities, it is still necessary to increase the reservoir condition, for instance to $T_0 \approx 2100$ K and $p_0 \approx 200$ bar, which can be realized by increasing the partial pressure of helium or using pure helium. More PIV experiments will be carried out in the near future for higher reservoir conditions and different particles in size and material.

In this study, a quite large facility is used allowing a better flow visualization and measurements. For real industrial applications, a much smaller spray facility is needed, which means a smaller nozzle and also a smaller volume of working gas. Furthermore, in order to build up a thick coating layer using this technique, an intermittent operation is necessary, which is under development at the Shock Wave Laboratory of RWTH Aachen University.

Acknowledgments

The authors gratefully acknowledge the financial support extended by the Deutsche Forschungsgemeinschaft (DFG) under the Project scheme OL 107/10-2 ''The generation of high particle velocities by shock tube technology for coating applications'' and the support of the Institute of Surface Engineering (IOT) at RWTH Aachen University for providing the cut views of the coating samples.

References

1. E. Lugscheider, K. Bobzin, and R. Nickel, The Application of Advanced Fluid Flow Modeling in Thermal Spraying Process Simulation, *Proceedings of 2005 Business and Industry Symposium of the Spring Simulation Multiconference*, April 3-7, 2005 (San Diego), 2005 Simulation Councils Inc., p 13-18
2. H. Kreye, F. Gärtner, T. Schmidt, and T. Klassen, Cold Spraying—From Thermal Spraying to Kinetic Spraying, *Proceedings of the 7th HVOF Kolloquium, Erding 2006*, November 9-10, 2006, p 9-16
3. A.P. Alkhimov, A.N. Papyrin, V.F. Kosarev, N.I. Nesterovich, and M.M. Shushpanov, Gas-dynamic Spray Method for Applying a Coating, U.S. Patent 5 302 414, April 12, 1994
4. T. Stoltenhoff, H. Kreye, and H.J. Richter, An Analysis of the Cold Spray Process and its Coatings, *J. Therm. Spray Tech.*, 2002, **11**, p 542-550
5. T. Schmidt, F. Gärtner, and H. Kreye, New Developments in Cold Spray Based on Higher Gas and Particle Temperatures, *J. Therm. Spray Tech.*, 2006, **15**(4), p 488-494
6. F. Gärtner, T. Stoltenhoff, T. Schmidt, and H. Kreye, The Cold Spray Process and its Potential for Industrial Applications, *J. Therm. Spray Tech.*, 2006, **15**(2), p 223-232
7. M. Grujicic, C.L. Zhao, C. Tong, W.S. DeRosset, and D. Helfritch, Analysis of the Impact Velocity of Powder Particles in the Cold-gas Dynamic-spray Process, *Mater. Sci. Eng. A*, 2004, **368**, p 222-230
8. J. Pattison, S. Celotto, A. Khan, and W. O'Neill, Standoff Distance and Bow Shock Phenomena in the Cold Spray Process, *Surf. Coat. Technol.*, 2008, **202**, p 1443-1454
9. K.V. Klinkov, V.F. Kosarev, and M. Rein, Cold Spray Deposition: Significance of Particle Impact Phenomena, *Aerospace Sci. Technol.*, 2005, **9**, p 582-591
10. H. Assadi, F. Gärtner, T. Stoltenhoff, and H. Kreye, Bonding Mechanism in Cold Gas Spraying, *Acta Mater.*, 2003, **51**, p 4379-4394
11. T. Schmidt, F. Gärtner, H. Assadi, and H. Kreye, Development of a Generalized Parameter Window for Cold Spray Deposition, *Acta Mater.*, 2006, **54**, p 729-742
12. B. Jodoin, P. Richer, G. Bérubé, L. Ajdelsztajn, A. Erdi-Betchi, and M. Yandouzi, Pulsed-gas Dynamics Spraying: Process Analysis, Development and Selected Coating Examples, *Surf. Coat. Technol.*, 2007, **201**, p 7544-7551
13. X. Luo, G. Wang, and H. Olivier, Shock Tunnel Produced Cold Gas-dynamic Spray: Modeling and Simulation, *Proceedings of the 25th Int. Symposium on Shock Waves* (Bangalore, India), July 2005, p 733-738, 2006
14. K. Bobzin, E. Lugscheider, R. Nickel, D. Parkot, W. Varava, H. Olivier, and X. Luo, A New Concept of the Application of Shock Wave Technology in the Cold Gas Dynamic Spray Process, *J. Therm. Spray Tech.*, 2007, **16**(5-6), p 729-735
15. X. Luo, G. Wang, and H. Olivier, Parametric Investigation on Particle Acceleration in High Enthalpy Conical Nozzle Flows for Coating Applications, *Shock Waves*, 2008, **17**(5), p 351-362
16. H. Olivier, An Improved Method to Determine Free Stream Conditions in Hypersonic Facilities, *Shock Waves*, 1993, **3**(2), p 129-139
17. B. Esser, Die Zustandsgrößen im Stoßwellenkanal als Ergebnisse eines exakten Riemannlösers, PhD thesis, RWTH Aachen University, 1991